ORIGINAL RESEARCH ARTICLE

High-Precision Nonenzymatic Electrochemical Glucose Sensing Based on CNTs/CuO Nanocomposite

Mithra Geetha[1] · Muni Raj Maurya[1] · Somaya Al-maadeed[2] · Asan Abdul Muthalif[3] · Kishor Kumar Sadasivuni[1]

Abstract

The measurement of blood glucose levels is essential for diagnosing and managing diabetes. Enzymatic and nonenzymatic approaches using electrochemical biosensors are used to measure serum or plasma glucose accurately. Current research aims to develop and improve noninvasive methods of detecting glucose in sweat that are accurate, sensitive, and stable. The carbon nanotube (CNT)-copper oxide (CuO) nanocomposite (NC) improved direct electron transport to the electrode surface in this study. The complex precipitation method was used to make this NC. X-ray diffraction (XRD) and scanning electron microscopy were used to investigate the crystal structure and morphology of the prepared catalyst. Using cyclic voltammetry and amperometry, the electrocatalytic activity of the as-prepared catalyst was evaluated. The electrocatalytic activity in artificial sweat solution was examined at various scan rates and at various glucose concentrations. The detection limit of the CNT-CuO NC catalyst was 3.90 μM, with a sensitivity of 15.3 mA cm^{-2} μM^{-1} in a linear range of 5–100 μM. Furthermore, this NC demonstrated a high degree of selectivity for various bio-compounds found in sweat, with no interfering cross-reactions from these species. The CNT-CuO NC, as produced, has good sensitivity, rapid reaction time (2 s), and stability, indicating its potential for glucose sensing.
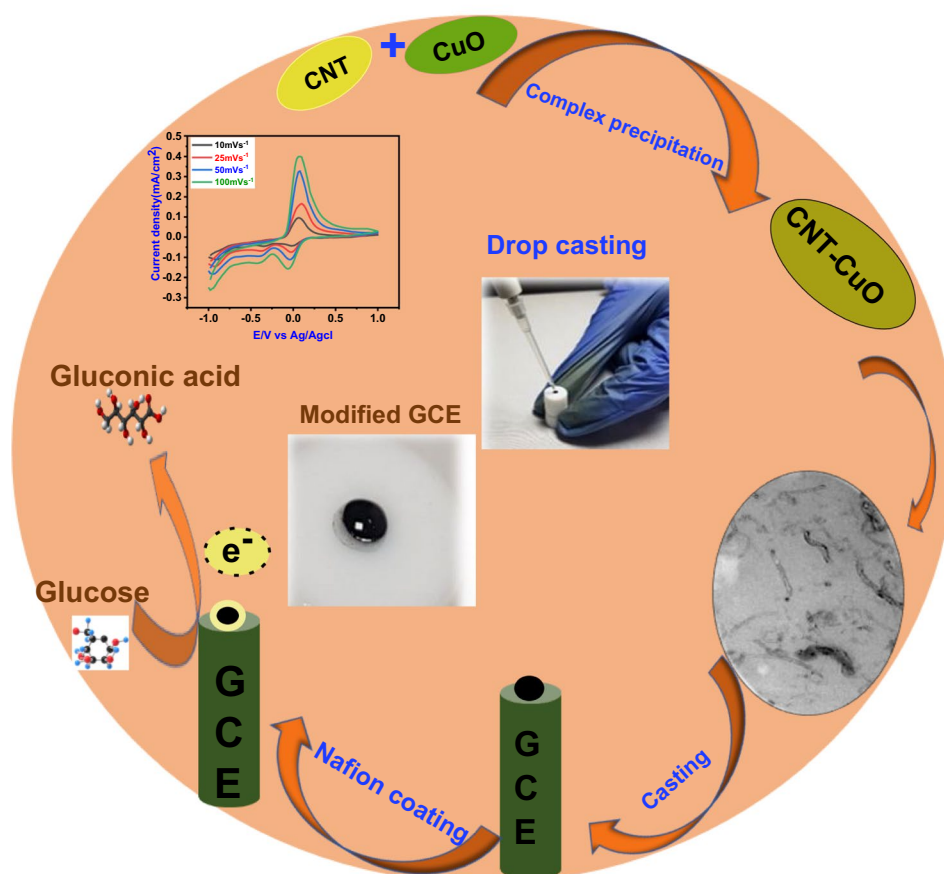
✉ Kishor Kumar Sadasivuni
kishor_kumars@yahoo.com

[1] Center for Advanced Materials, Qatar University, P.O. Box 2713, Doha, Qatar

[2] Department of Computer Science and Engineering, Qatar University, P.O. Box 2713, Doha, Qatar

[3] Department of Mechanical and Industrial Engineering, Qatar University, P.O. Box 2713, Doha, Qatar

Graphical Abstract

Keywords Carbon nanotube · sensors · nanocomposite · chronoamperometry · electrocatalysis

Introduction

Glucose monitoring is, of course, largely associated with diabetes, a chronic metabolic condition characterized by abnormal blood glucose levels. According to a recent estimate by the World Health Organization (WHO), this ailment affects over 422 million people worldwide and is the third greatest cause of mortality.[1] Because most diabetics do not identify early indicators of diabetes and ignoring it has serious consequences, frequent blood glucose monitoring and sensitive detection are essential for diagnosing and controlling this life-threatening condition. Glucose concentration has mostly been evaluated in whole blood, plasma, and serum for the past five decades.[2] Each sampling requires the skin to be punctured, which is cumbersome if several repeats are required. Infections can also be spread by direct blood contact.[3] Because of the sampling method (finger pricking), continuous glucose concentration measurements using blood glucose test strips are not practicable; hence, implanted sensors have been proposed.[4] The low detection limit possible with electrochemical techniques opens the possibility of developing glucose detection methods for human tissues and fluids other than blood. Body fluids that are constantly generated and discharged, such as urine, saliva, sweat, tears, or exhaled air, can be utilized to detect the amount of glucose concentration in blood.[5] Human sweat glucose concentrations range from 0.01 mM to 0.1 mM, while diabetes individuals' sweat glucose concentrations exceed 0.5 mM.[6] Electrochemical sensors have acquired popularity in the context of quick diagnosis due to their low cost, ease of preparation, sensitivity, rapid response, and simple operation that allows for individual self-monitoring.[7]

The majority of commercially available glucometers are enzyme-based due to their high sensitivity and selectivity for the analyte. The glucose oxidase enzyme mounted on the electrode surface is a common sensing element in

electrochemical glucose sensors.[8] The first-generation glucose sensors measured the signal by measuring the oxygen concentration at the electrode, but the second-generation sensors employed a redox mediator. Third-generation sensors used direct electron transfer at the electrode surface to measure current. However, electron transport from the immobilized enzyme to the electrode surface was sluggish, and enzymatic sensors are restricted by their instability due to temperature and pH fluctuations. This inspired the creation of nanostructured surfaces that allowed for faster electron transfer.[9] As a result, the fourth generation of enzyme-free electrochemical sensors has been developed. Nano-dimensional particles on the electrode surface catalyze the reaction. The nano-interface has a high surface-area-to-volume ratio, allows for quick and direct electron transport, has good electrical and mechanical characteristics, and may adsorb biomolecules (Table I).[10]

Optical, enzymatic, and electrochemical methodologies are used to classify the described nanoparticle-based glucose detection systems. The creation of a complex between the recognition element and the target determines the reflective index change of the transducer in optical nanoparticle-based sensors. Direct optic nanoparticle-based sensors generate signals via a complex formation on the transducer surface, while indirect optic nanoparticle-based sensors generate signals via a complex formation on the transducer surface. The indirect optic nanoparticle-based sensors, on the other hand, are primarily developed with various labels to assess the binding and expand the signal. The electrochemical sensors' primary premise is that they react with chemical solutions and provide an electrical signal proportional to the analyte concentration. Nanoparticles have a number of unique traits that can be used to create biosensors with desirable characteristics such as increased sensitivity and lower detection limits. Because current biomolecule detection methods are insufficient, the development of highly sensitive sensors with detection capabilities of less than 10 parts per billion (ppb) = 10 nmol mol^{-1} is critical for early detection

of these agents, allowing for their neutralization or control through appropriate countermeasures. As a result, hand-held instruments require compact, low-power sensors to detect qualitatively without causing false alarms. The biomolecule must also be quantified, which necessitates the use of sensors. Nanoparticles have unique features that separate them from bulk materials, owing to their huge surface area, which favors surface qualities over bulk properties.

Because the electrode surface plays such an essential role in fabricating non-enzymatic glucose detectors, synthesizing a catalyst with porous structures is critical. The high number of active sites, high permeability, and a shorter charge transfer channel length are benefits of micro/nanoporous morphologies, which are attractive for sensor applications. Carbon nanotubes (CNTs) are made up of layers of carbon atoms organized in six-membered rings. Porosity is formed by an amorphous structure of aromatic sheets and strips with slits of varying molecular diameters. CNTs are made up of curved sp^2-hybridized carbon atoms stacked in concentric cylindrical planes in an axial orientation.[18] The oxygen functional groups on the supports have been important in defining their uses.[19] On the other hand, CuO is a non-toxic n-type semiconductor compound with a narrow band gap (1.21–1.51 eV), excellent permeation, high number of active sites, large surface area, and strong electrical characteristics that can improve the electrochemical properties of CNT. Furthermore, by synthesizing the NC of CNT and CuO, porous morphologies of the catalyst may be obtained. The NC creation produces a morphology with a high surface-to-volume ratio, which improves the material's electrocatalytic activity.[20] The usage of carbon nanotubes in combination with CuO nanoparticles has been discovered to improve electron transport while the metallic centers carry out the catalysis. As a result, this study looked at the prospect of using CNT-coupled CuO's electrocatalytic nature for glucose testing.

Current research aims to develop and improve noninvasive methods for detecting glucose in sweat making it easier

Table I Summary of sensors for different biological molecules

Detection mode	Sensor	Transduction principle	Sensor category	References
Optical	Carbohydrate-coated metal surface nanoparticles colour change	Plasmon absorption-based	Biosensor	11
Optical	Fluorescence-quenched sensors	Fluorescence quenching	Biosensor	12
Optical	Nanoparticle-modified fluorescence of enzyme inhibitor	Fluorescence intensity change	Biosensor	13
Electromagnetic	Magnetic nanoparticle-based sensor	Detection of generated frequency mixing components by the differentially wound pickup coil	Biosensor	14
Electrochemical	Zirconia nanoparticle-based sensor	Voltammetry	Chemical sensor	15
Electrical	Nanowire- or nanotube-based FETs	Resistance change	Chemical sensor	16
Electrical	Metal nanoparticle-based chemiresistor	Resistance change	Chemical sensor	17

to diagnose and manage diabetes. This study explores the possibility of using CNT-CuO as a catalytic interface for enzyme-free glucose measurement in an artificial sweat solution. The cyclic voltammetry (CV) response for various glucose concentrations was used to test the material's sensitivity. The synergistic consequence encouraged by electrical interactions among CNT/CuO NC plays a significant role in improving the electrocatalytic performance of this NC for efficient glucose detection. Electrodes made of CNT/CuO NC can be employed in wearable biosensors to monitor glucose levels in human sweat. Diabetes, atherosclerosis, diabetic retinopathy, renal failure, nerve degeneration, and other diseases can be reduced with proper glucose monitoring.[21]

Materials and Methods

Materials

D-Glucose (Hi-media), Nafion (M/s Sigma-Aldrich Ltd.), and CNTs (Nanomor, USA) were utilized in the study. Sodium dodecyl sulfate (SDS) and copper chloride (CuCl$_2$) were procured from (M/s Sigma-Aldrich Ltd.). The glassy carbon electrode (GCE), KCl saturated Ag/AgCl reference electrode, and graphite rod counter electrodes were purchased from CH Instruments Inc., USA, and used for the electrochemical measurements. Sodium hydroxide (NaOH, 98%) was purchased from Scharlau. Glucose (99%), lactose (99%), fructose (99%), uric acid (99%), ascorbic acid (99%) and fructose (99%) were purchased from Fisher Scientific. Avonchem provided sodium chloride (NaCl, 99%). Urea (98+%), lactic acid (85–90% aqueous solution), potassium chloride (KCl, 99%), and ascorbic acid (99%) were purchased from Alfa Aesar. The experimental solutions were synthesized with double-distilled water as the solvent.

Synthesis of CNT/CuO NC

A mixture of CNTs, SDS, and CuCl$_2$ was dispersed in 50 mL distilled water for 30 min. The solution was then amended with excess aqueous ammonia. The solution was treated with NaOH drop by drop and stirred at 50°C for another 1 h. The sample was filtered, washed several times with distilled water, dried, and calcined in a muffle furnace for 2 h.[22]

Fabrication of the CNT/CuO NC Modified Electrode and Artificial Sweat Solution

To prepare the catalytic ink, 25 mg of CNT/CuO NC was mixed with 0.5 mL of ethanol and 40 μL Nafion (proton conductor). The resultant mixture was sonicated for 1 h in an ice bath. The homogeneous suspensions obtained after ultrasonication were drop-cast on the GCE and dried at room temperature. Artificial sweat solution was prepared using 22 mM urea, 5.5 mM lactic acid, 25 mM of uric acid, and 10 mM of KCl.[23]

Characterization Techniques

The prepared CNT/CuO NC was evaluated in morphology and structure. The crystal structure was studied using an x-ray diffractometer (X'PERT-Pro MPD, PANalytical Co., Almelo, Netherlands). TESCAN Mira3 was used to obtain SEM and elemental mapping data. TEM was carried out using FEI, Model Tecnai G2 S Twin F20. At a 3-kV accelerating voltage, the sample was sputter-coated with a thin coating of gold and imaged. To verify the chemical bonding of the materials, Fourier transform infrared (FT-IR) spectra were measured on a Nicolet 740 spectrometer using pressed KBr pellets from 100 cm^{-1} to 4000 cm^{-1}. Using a three-electrode cell configuration, a Gamry potentiostat/galvanostat (Ref 600) was employed for cyclic voltammetry (CV) and chronoamperometry testing. Graphite, Ag/AgCl (3M KCl solution), and GC were used as the counter, reference, and working electrodes, each with a diameter of 5 mm.

Results and Discussion

Structural and Morphological Analysis of CNT/CuO NC

x-ray diffraction spectroscopy is a non-destructive method for determining crystal structure, interlayer spacing, sample purity, and structural defects. Diffraction spectra generated by x-ray scattering characterize CNT.[24] The XRD patterns of as-synthesized CNT/CuO NC are shown in Fig. 1.
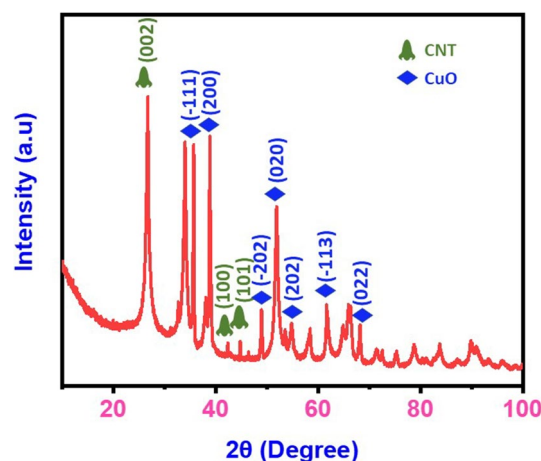

Fig. 1 XRD pattern of CNT-CuO NC.

According to the XRD data, the CNT/CuO NC confirms the phases of monoclinic CuO and cubic CNT.

The XRD patterns obtained at $2\theta = 35.4°$ (-111), $2\theta = 38.8°$ (200), $2\theta = 48.7°$ (-202), $2\theta = 52°$ (020), $2\theta = 58.3°$ (202), $2\theta = 61.6°$ (-113), $2\theta = 65°$ (022), belong to the CuO nanoparticles (NPs) and are well in agreement with standard JCPDS card number 89-2531. When compared to the x-ray incident beam, CNT exhibits numerous orientations. The distribution of diameters and chiralities is also observed, leading to statistical characterizations of CNTs. The major characteristics of the XRD pattern of CNTs are similar to those of graphite due to their intrinsic nature. Peak (002), which resembles graphite, is always present. A family of peaks may also be present due to the honeycomb lattice of a single or many graphite sheets. The observed peaks at $2\theta = 26.4°$ (002), $2\theta = 43.0°$ (100), $2\theta = 43.8°$ (101) correspond to the cubic phase of CNT (JCPDS 26-1076) and these peaks correspond to the inter-shell spacing of the concentric cylinders of graphitic carbon (CNT). According to the diffraction studies, the structure of as-prepared CNT is found between the chaotic amorphous carbon and highly ordered graphitic phases.[25] The Debye–Scherrer equation was used to compute the crystallite size.[26] The study determined the average crystallite size of CNT/CuO NC to be ~ 30.12 nm. The diffraction peaks are widened, indicating that the NC as-synthesized is polycrystalline.

An inference of the preparation of CNT/CuO is presented below. CNTs were functionalized with carboxylic and hydroxyl groups, as reflected by the bands at 1719 cm^{-1} and 2439 cm^{-1}. A [Cu (NH$_3$)$_4$]$^{2+}$ complex was formed upon adding superfluous NH$_3$·H$_2$O. CNTs were attached to [Cu (NH$_3$)$_4$]$^{2+}$ via amide and carboxylic reactions.[27] This can be proved as no band corresponding to the carboxylic groups can be detected in the FTIR spectra of CNT/CuO NC. Cu (OH)$_2$ precipitate was generated in situ when NaOH solution was slowly added, and it was stabilized via chemisorption and van der Waals interactions between Cu (OH)$_2$ and CNTs.[28] Cu (OH)$_2$ was transformed to CuO under heating and stirring conditions. The color of the solution changed from blue-green to blue, then black, throughout the preparation process of pure Cuo nanoparticles, which can help confirm the production process of CNT/CuO stated above to some extent. The as-prepared NC's useful vibration characteristics were further investigated.

Under standard circumstances, FTIR spectra were obtained in the range of 100–4000 cm^{-1}. Figure 2 displays the vibrational bands in the FTIR spectra of CNT-CuO. The O-H stretching mode was responsible for the peak at 1479 cm^{-1}. The bands at 1386 cm^{-1} were ascribed to the C-O stretching vibration,[29] while the peak at 2458 cm^{-1} was attributed to CO$_2$ physiosorbed on the surface of the materials.[30] Cu-O bond bending was visible in the absorption band at 523 cm^{-1}.[31] Furthermore, the XRD and FTIR
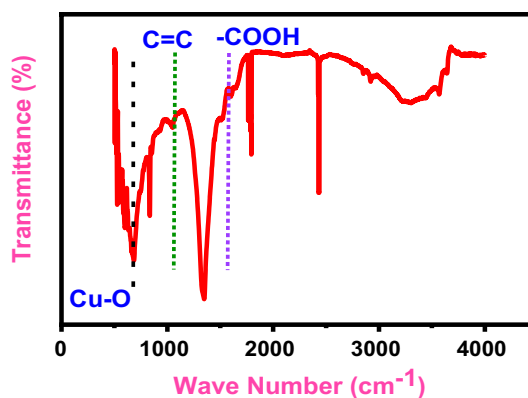

Fig. 2 FT-IR spectra of the prepared CNT/CuO NC.

examination of NC revealed no impurity peaks, indicating that high purity CNT/CuO NC was effectively synthesized through the complex-precipitation method.

The SEM picture of CNT/CuO in Fig. 3a reveals CuO nanoparticles well scattered over the CNT surface. This picture also shows the scattered dispersion of CuO nanoparticles on CNTs. Although the SEM specimen has been subjected to long-term sonication, scattered loading of CuO nanoparticles on CNTs can still be visible.[32] According to the SEM pictures, the nanoparticles were consistently formed, and the crystallite structure was uniformly organized on the surface. The nanostructured features of each particle could be seen in the SEM micrograph. The nanoporous character of the synthesized particles has also been represented by the integration of nanoparticles to produce the final micron-sized particles, as shown in the SEM image. The inclusion of surfactant in the synthesis technique may have contributed to creating nanoporous surfaces. Some of the particles have holes, indicating that they are hollow. The porous morphology is well dispersed over the surface of the CNT/CuO NC, as seen in the picture. The presence of a porous structure on the surface of NC is favorable because it increases surface permeability and enhances adsorption efficacy. It also allows charge carriers to be swiftly transferred to the particle surface, substantially lowering the carrier recombination rate and speeding up surface reactions. Figure 3b shows the TEM image of the CNT/CuO NC. From the TEM image the scattered deposition of CuO on the CNT is evident. The wire-like morphology in Fig. 3b represents the CNT, and dark spots indicated by the arrow represent the CuO nanoparticles deposited on the CNT surface. The SEM and TEM results are consistent with the XRD results.

Electrochemical Profile of Glucose on CNT/CuO NC

Cyclic voltammetry (CV) experiment for the CNT/CuO NC tailored GCE in artificial sweat solution was done to
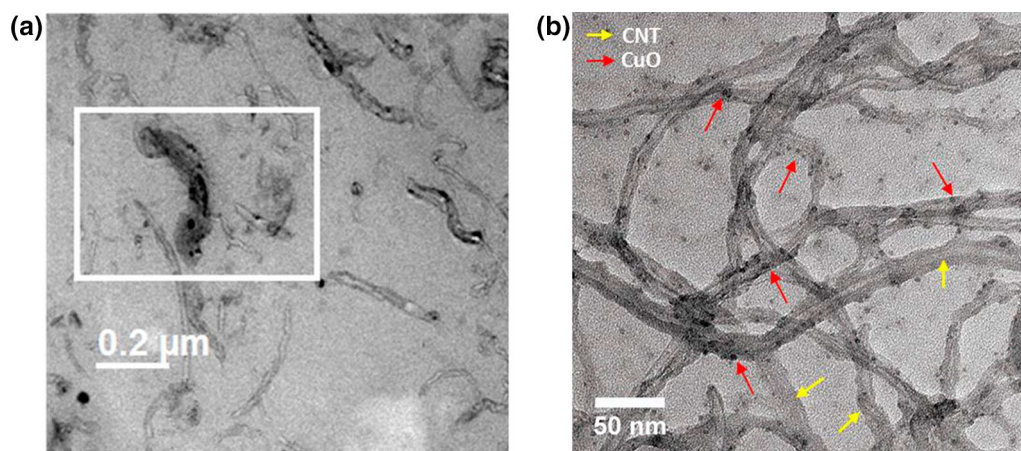
Fig. 3 (a) SEM image, (b) TEM image of CNTs/CuO NC, respectively.

investigate the efficacy of the CNTs/CuO NC tailored GCE electrode. The electrochemical kinetics of the CNTs/CuO NC modified electrode for glucose detection utilizing CV analysis are shown in Fig. 4. Figure 4a shows the CV curve for a CNTs/CuO NC modified electrode with and without 50 mM glucose at a scan rate of 25 mV s^{-1}, which shows that there are no apparent redox peaks with a glucose-depleted electrolyte. It is worth noting that in the presence of 50 μM glucose, the current density of the CNT/CuO NC modified electrode increases to 0.39 mA cm^{-2} and −0.15 mA cm^{-2} at 0.16 V and −0.02 V, respectively.

Furthermore, the CNT/CuO NC modified electrode CV curves indicate better current density and increased loop area in the presence of glucose. The oxidation of glucose occurs at a lower potential,[33] as shown in Fig. 4a, and the presence of a strong redox peak in the CNT/CuO NC modified electrode confirms the as-synthesized NC's high electrocatalytic performance for glucose detection.[34] Figure 4b illustrates that the oxidation peak maintains its location regardless of scan rate changes. On the other hand, for higher scan speeds, the current density is increased, which demonstrates that the CNT/CuO NC has good catalytic activity for glucose detection.[35]

The increase in current density was further investigated by graphing the cathodic and anodic peak current density in relation to the square root of scan rate, as shown in Fig. 4c. The plot of the current density displays a linear connection with respect to the square root of the scan rate, regardless of the oxidation or reduction cycle. This shows that the electrochemical reactions were governed by the rate at which the electrolyte diffused to the active sites. Furthermore, the linear connection shows that adsorption-controlled activity was involved in glucose oxidation.[36] The CNT-CuO NC catalyst's electrochemically active surface area (EASA) was calculated using the scan rate dependence of cyclic voltammetry experiments given in Fig. 4 and the double-layer

capacitance (Cdl) measurement of the CNT-CuO NC catalyst. As illustrated in Fig. 4d, the Cdl was computed by graphing the current density difference ($\Delta J = Ja–Jc$) between anodic and cathodic sweeps against the scan rate. Because the fitted linear regression slope equals twice the Cdl, the Cdl of the CNT-CuO NC catalyst was determined to be 18.3 mF cm^{-2}, indicating a high density of the electrochemically active surface area. The EASA was then calculated using the equation EASA = Cdl/Cs. Cs denotes the specific capacitance of conventional electrode materials on a unit surface area. According to the literature, a typical Cs value of 0.02 mF cm^{-2} was used in the computation[37,38] resulting in EASA = 915. According to the CV study, the CNT-CuO NC has a considerably large number of active sites, excellent electrical characteristics, quick analyte transit kinetics, and is extremely sensitive for the detection of glucose. The modified electrode surface constrained electrochemical redox process is indicated by the calibration plot of the square root of the scan rate and the peak current.

The conversion of glucose to gluconic acid, aided by the CNTs on the electrode surface, causes the oxidation peak in the CNT/CuO coated GCE (Fig. 5). Earlier research has shown that glucose oxidation may occur in an alkaline medium, with electron transport mediated by CNT and unaffected by chloride ions in the medium.[31] Rather than using sodium hydroxide, which includes chloride ions, as the electrolyte in previous studies, the current study used artificial sweat, which also contains chloride ions. Although the specific mechanism for CNT/electrocatalytic CuO's activity is unknown; it is thought that a combination of defect sites at the cap and the presence of oxygen-containing functional groups contribute to CNT/CuO electrocatalytic effect.[39]

Furthermore, surface roughness helps to improve the sensitivity of the CNT/CuO modified surface to the analyte. The faulty sites in CNTs enable the adsorption of the hydroxyl ions that catalyze the oxidation of glucose to gluconic acid,
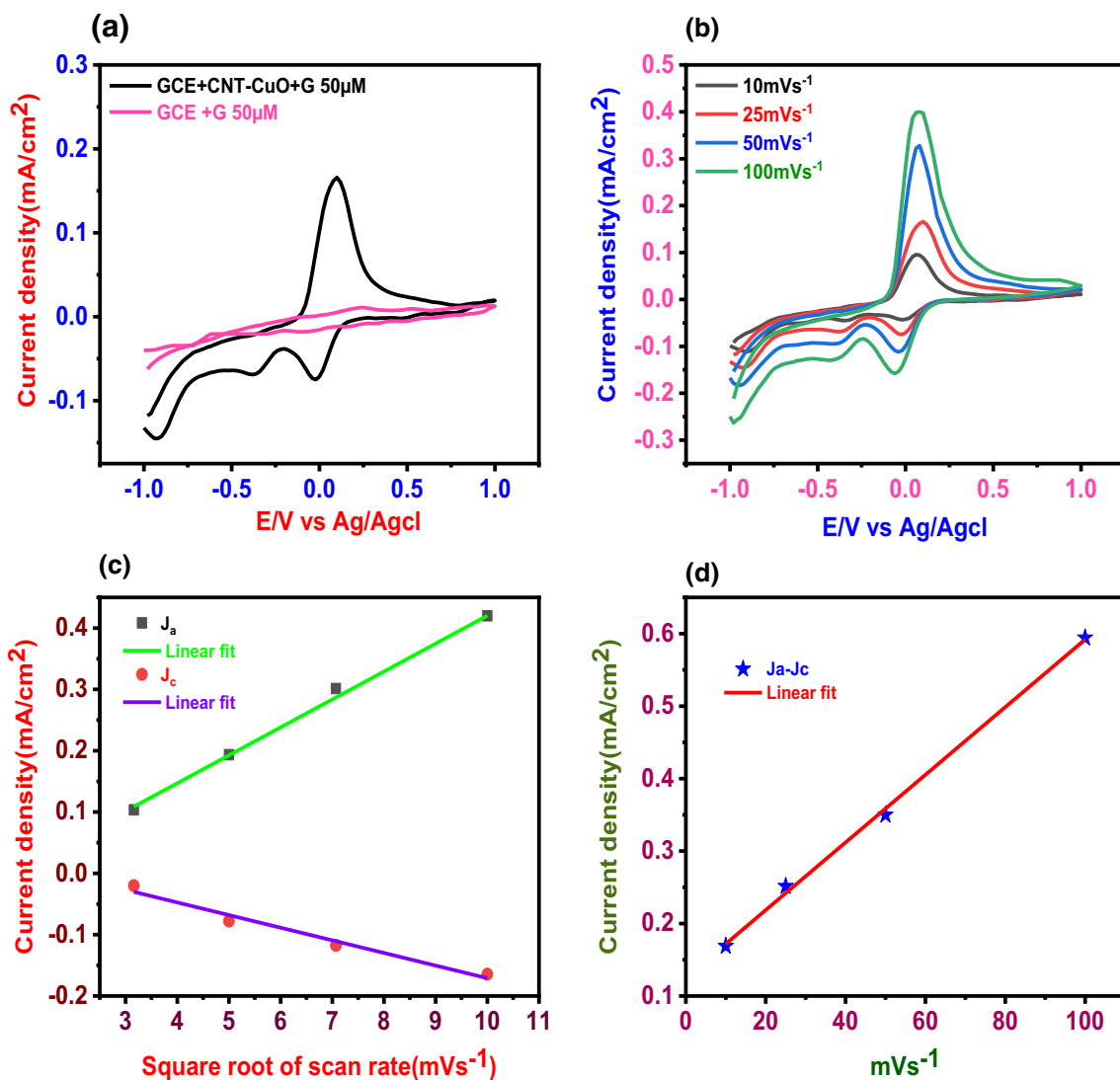
Fig. 4 CV analysis of CNT/CuO tailored GCE electrode. (a) CV response of CNT/CuO modified GCE electrodes with and without the presence of 50 μM glucose. (b) CV measurement of CNT/CuO tai-lored GCE electrode at different scan rates. (c) Graph of redox peak current density with respect to the square root of the scan rate. (d) Linear fitting of the current density differences against scan rates.
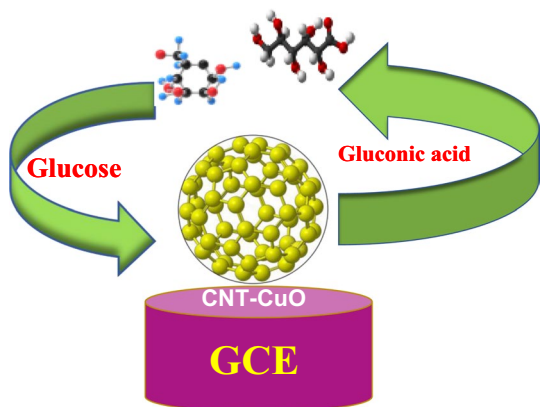

Fig. 5 Schematic representation of the reaction occurring at the CNT-CuO modified GCE.

according to the Incipient Hydrous Oxide Adatom Mediator model (IHOAM).[40] The presence of trace quantities of metal catalyst utilized to prepare CNT/CuO in the catalytic transformation, on the other hand, cannot be ruled out. The Nafion covering prevents bigger molecules from diffusing, reducing interference. In the presence of glucose, the peak current displays a gradual rise, increasing scan rates. The fact that the scan rate and current are linearly related suggests that the oxidation reaction is restricted to the electrode's surface. The oxidation and reduction peaks' linear response as scan rate and concentration increase validates the diffusion-controlled electron transfer mechanism.[41]

The sensitivity of the CNT/CuO NC was further studied by altering the glucose concentration from 5 μM to 100 μM. Increased glucose concentrations were used to assess the

concentration-dependent response of the produced CNT-CuO NC on glucose (Fig. 6). The redox peak potential was measured at 0.16 V and −0.02 V, and the redox peak current density increased as the glucose concentration increased. It was discovered that as the glucose concentration increased, the current increased as well. A linear trend with a positive slope and linear regression of 0.998 can be seen in the plot of concentration against the current density. This clearly shows that the oxidation process at the CNT-coated GCE is a surface-controlled phenomenon.

Furthermore, the linear increase in cathodic and anodic peak current density with increasing glucose loading reveals the CNT/CuO NC's great sensitivity to glucose detection.[42] It also suggests that the CNT-CuO NC contains many active sites, which aids in the high rate of electron transport. The

reversible character of the electron transfer mechanism is confirmed by the linear intensification of the peak current with concentration. The exceptional sensitivity of the CNT-CuO NC in detecting glucose is due to surface chemical reactions occurring at low ionization potential. As a result, the transport of electrons in the redox reaction is accelerated, resulting in high redox current values. The redox couple Cu^{2+}/Cu^{3+} may be responsible for the reported redox peaks.

Nearly linear increase in the peak current is noticed with the increase in glucose loading, which confirms that the electron transfer is a reversible process (Fig. 6b). The variation of peak current density with respect to the glucose concentration is shown in Fig. 6b. Limit of detection (LOD) was calculated using the $3\sigma/m$ criterion, where m represents the slope of the calibration plot, and σ is the standard
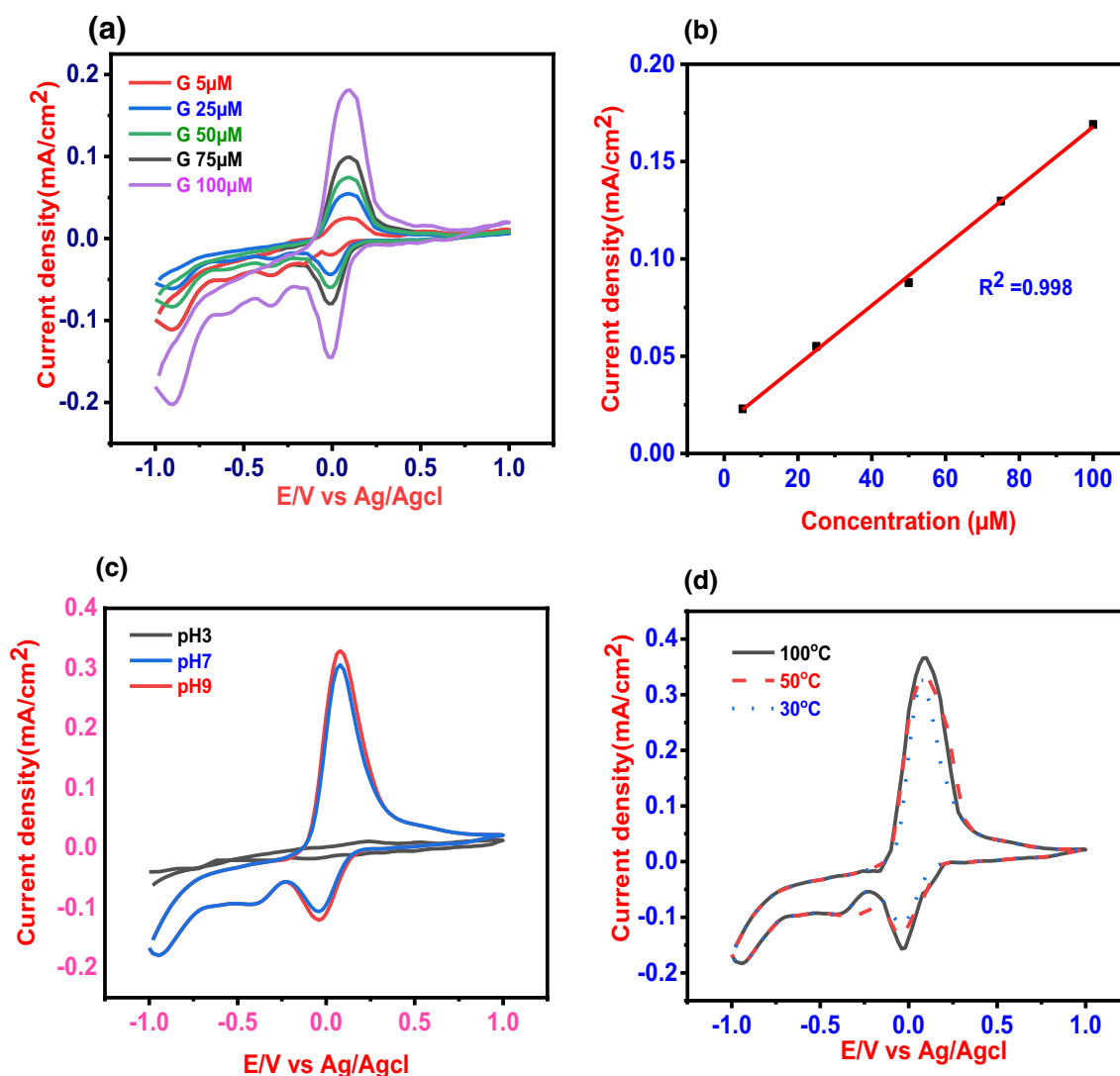

Fig. 6 (a) CV response of CNT/CuO towards different glucose concentrations at a scan rate of 10 mV s^{-1}. (b) Calibration curve in the linear range of 5–100 μM. (c) CV curve of CNT-CuO NC at different pH levels. (d) CV plot of CNT-CuO NC in pH 7 sweat solution at different temperatures.

deviation of the intercept. The estimated LOD of glucose in the artificial sweat solution was 3.90 μM ($y = (0.0153)$ $x + (0.0149 \pm 0.00199)$; $R^2 = 0.998$). The sensor showed a sensitivity of ~ 15.3 mA cm^{-2} μM^{-1} in a linear range of 5–100 μM and a response time of ~ 2 s. This indicates that the CNs-CuO NC exhibits high surface area as well as enhanced conductivity, which synergistically improves the electrocatalytic activity towards glucose sensing.

One of the most significant qualities for sensing applications is its resistance to changes in the surrounding or involved medium's parameters. Figure 6c depicts the CNT-CuO NC's CV response in varied pH sweat solutions (pH 3 (acidic), pH 7 (neutral), and pH 9 (alkaline)). For pH 7 and pH 9, there is no substantial change in current density when glucose is added. Thus, the CNT-CuO NC is stable for glucose detection in the neutral and alkaline medium, while no redox reaction occurs in the acidic solution. Consequently, pH values of 7 and 9 do not affect the performance of the as-synthesized glucose-detecting NC. Similar research on the influence of pH on electrode sensitivity has revealed that raising the pH boosts the catalyst sensitivity to glucose. The additional electrons were transferred to the Cu^{2+}/Cu^{3+} redox couple by the reduced species, increasing the redox current. It is worth noting that alkaline conditions on the electrode surface can reduce ion contamination limitations because the hydroxyl groups (OH) inhibit chloride (Cl) adsorption to the electrode surface.[43–45] As a result, adjusting the true pH of the sweat solution greatly improved the sensitivity of the as-prepared electrode in this study. Previous studies have reported on the remarkable catalytic activity of transition metal oxides such as CuO in alkaline solutions for glucose detection.[46] Unlike more expensive noble metals, these transition metal oxides are less influenced by interfering species and are more cost-effective.[47–49] The voltammetry peak was not visible at CNTs-CuO NC in acid electrolyte, as shown in Fig. 6c. Earlier research has shown that glucose oxidation may occur in alkaline medium and that electron transport is mediated by the presence of CNT and is unaffected by the presence of chloride ions in the medium.[50] While previous studies used sodium hydroxide with chloride ions as the electrolyte, the current study followed the same strategy but used moderately alkaline and neutral artificial sweat. The emergence of the glucose oxidation peak suggests that the fake sweat's moderately alkaline and neutral environment is adequate for the oxidation of glucose to gluconic acid, which is catalyzed by the CNT-CuO modified surface, which also efficiently captures the consequent electron transfer. Although the specific mechanism for this NC's electrocatalytic action is unknown, it is thought that a combination of defect sites at the cap and the presence of oxygen-containing functional groups contribute to the electrocatalytic effect.[51]

It is important to consider the influence of temperature on sensitivity while developing a real-time biosensor implementation. Figure 6d demonstrates how temperature affects the performance of a CNT-CuO NC electrode in a sweat solution with a pH of 7. As shown in Fig. 6d, the CV curve shows a modest divergence in current density over a large range of temperatures of 30°C, 50°C, and 100°C. According to the temperature study, temperature has little influence on the rate of redox pair reactions. According to the findings, the CNT-CuO NC biosensor has good temperature stability, which is critical for real-time glucose detection from human sweat.

Selectivity, reproducibility, repeatability, and stability are key factors in evaluating sensing devices. Lactose, sucrose, fructose, uric acid, and acetic acid are readily oxidizable substances that coexist with glucose in human sweat. As a result, amperometric measurement of various oxidizable chemicals in relation to glucose concentration is carried out to determine the selectivity of the CNT-CuO NC, as shown in Fig. 7a. Based on Fig. 7a, it is evident that lactose, fructose, sucrose, uric acid, and acetic acid do not cause significant interference. As a result, the CNT-CuO NC is extremely selective for glucose detection instead of interacting with other species in the sweat. The lack of incompatibility between subsequent readings using the same electrode is repeatability. Three times in 1 day, a single modified GCE was used to test the repeatability. Figure 7b displays the RSD of the repeatability, which is 2.07%, indicating that the suggested sensor has excellent repeatability.

The proximity of findings obtained using a number of the same modified electrodes and the same measuring technique is referred to as reproducibility. At the ideal condition, the CV responses of three separate electrodes were recorded after each addition of 100 μM glucose. The response currents for distinct CNT-CuO NC electrodes had a relative standard deviation (RSD) of only 1.07%, indicating high consistency and accuracy (Fig. 8a). The electrode response was measured in the presence of 100 μM glucose in artificial sweat solution at a scan rate of 100 mV s^{-1} to determine its long-term stability. By storing the CNT-CuO NC modified GCE electrodes in air and monitoring the current response of 100 μM glucose, the durability of the proposed electrochemical sensor was assessed. Figure 8b shows that after keeping CNT-CuO NC modified GCEs in the air for 15 days, the response current of 100 μM glucose could preserve around 95.96 % of its initial value, showing good storage stability. From the time the sensor is added to the electrolyte, it takes a certain amount of time to create a steady condition of sensor reaction toward the substrate. After adding the sample to the sensor, it took 2 s to reach a steady current (Table II).
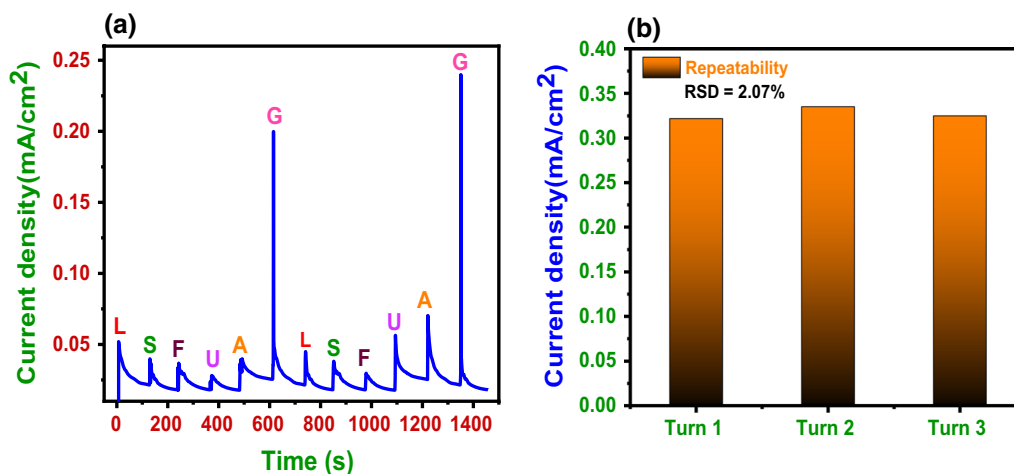
Fig. 7 (a) The chronoamperometric response of the CNT-CuO NC sensor after addition of 100 μM lactose, sucrose, fructose, uric acid, acetic acid and glucose in artificial sweat solution at 0.16 V (Ag/AgCl). (b) Repeatability of the cyclic voltammetric analysis of CNT-CuO NC sensor after addition of 100 μM glucose in artificial sweat solution.
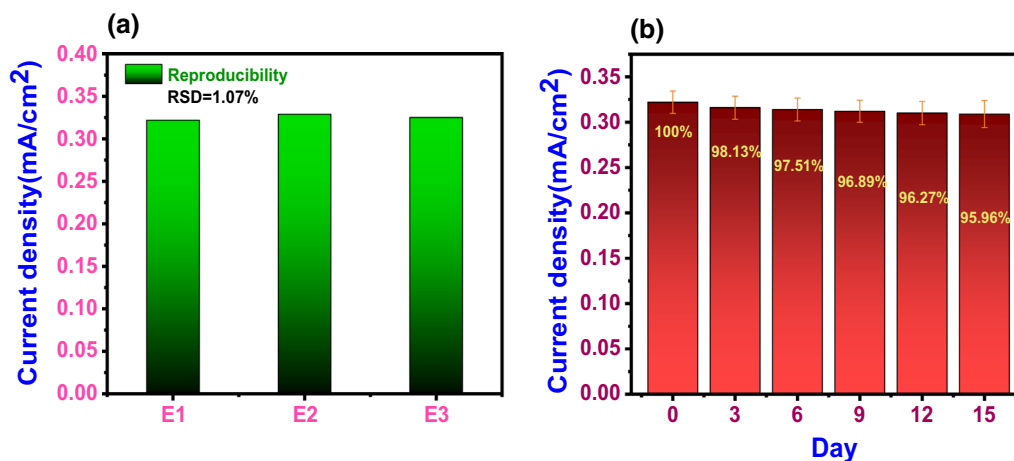

Fig. 8 (a) Reproducibility and (b) stability of the CNT-CuO NC sensor after addition of 100 μM glucose in artificial sweat solution.

Conclusions

CNTs and CuO were used in the current study to demonstrate the catalytic activity of the nanocomposite in the detection of glucose in artificial sweat as an electrolyte. Detailed analysis of the CNT-CuO NC for glucose sensing was performed. The complex precipitation method was used to create the CNT-CuO NC successfully. This NC established a catalytic interface for effective electrochemical enzyme-less glucose detection due to its outstanding electron transport capabilities. The CNT-CuO NC organization was revealed by XRD, with an average crystallite size of 30.12 nm. Morphological investigations revealed that the CNT-CuO NC with porous surfaces were homogeneous and well defined. CuO surface functional groups were confirmed by using FT-IR. Cyclic voltammetry and chronoamperometry were used to test CNT-CuO NC glucose-sensing ability. According to electrochemical measurements, the CNT-CuO NC catalyst has a detection limit of 3.90 μM with the sensitivity of 15.3 mA cm^{-2} μM^{-1} in the linear range of 5–100 μM. In artificial sweat solution, the CNT-CuO NC has excellent sensitivity, selectivity, quick response, and stability for glucose detection. In light of the glucose-sensing capabilities of CNT-CuO NC, it is a suitable material to incorporate into wearable sensor devices for glucose sensing in the detection and reduction of diabetes risk, preventing heart disease, diabetic retinopathy, kidney failure, and nerve degeneration.

Table II Studies performed where CNT/CuO nanocomposite is used as glucose and/or biosensors

Enzymatic glucose sensors	Sensitivity	Linear range	Detection limit	Reproducibility (%)	Lifetime	Ref.
GOx/Pt-DENs/PANI/CNT	42.0 µA mM^{-1} cm^{-2}	1 µM–12 mM	0.5 µM	4.7	3 weeks	52
Pt-DEN/GOx)$_4$/CNTs	30.64 µA mM^{-1} cm^{-2}	5 µM–0.65 mM	2.5 µM	2.3	30 days	53
NiCoO$_2$/CNT	1424.41 µA mM^{-1}	10 µM–6.5 mM	1.14 µM	3.7	2 weeks	54
ERGOc–MWCNTd/GOx/	7.95 µA mM^{-1} cm^{-2}	0.01–6.5 mM	4.7 µM	205	1 month	55
TiO$_2$/CNT/Pt	0.24 µA mM^{-1} cm^{-2}	0.006 mM–1.5 mM	5.7 µM	4.8	1 month	56
CuO/rGO/CNT	9278 µA mM^{-1} cm^{-2}	10–1000 µM	1 µM	4.1	4 weeks	57
GR-CNT-ZnO	5.362 ($\pm$0.072) µA mM^{-1} cm^{-2}	10 µM–6.5 mM	4.5 µM	3.24	4 weeks	58
Au/POAP/CNT/GO	11.4 mA M^{-1} cm^{-2}	10 mM	0.01 mM	8.4	30 days	59
Ag NPs/ZIF-67/CNT	469.4 µA mM^{-1} cm^{-2}	0.01–1.0 mM	0.46 µM	4.01	28 days	60
GR-CNT-ZnO-GOx	5.36 ($\pm$0.072) µA mM^{-1} cm^{-2}	0.01–6.5 mM	4.5 µM	3.24	4 weeks	61
CNT@GO/Ni(OH)2-	0.75 µM	5–1100 µM	40 nA	2.8	4 weeks	59
Graphene/CNT composite	53.89 µA mmol L^{-1} cm^{-2}	0.004–5 mmol L^{-1}	3.99$\times$10^{-7}mol L^{-1}	1.9	2 weeks	62
GR-MWNTs/AuNPs	0.695 µA mM^{-1} cm^{-2}	10 µM – 2 mM	4.1 µM	1.86	2 months	63
Cu–Gox/CNTPE	(2.544$\pm$0.008) 10^4 nA M^{-1} cm^{-2}	1.20$\times$10^{-2} M	2.0$\times$10^{-5} M	12.0	2 months	64
Present work	15.3 mA cm^{-2} µM^{-1}	5–100 µM	3.90 µM	1.07	6 months	65

Conflicts of intrest
The authors declare that they have no conflict of interest.

References

1. S.L. Smith and R. Gorantla, Analysing the Global Health Agenda: A Comparison of Priority for Diabetes and Oral Diseases. *Glob. Public Health* 16, 517 (2021).

2. R. Haeckel, W. Wosniok, A. Torge, R. Junker, A. Bertram, A. Krebs, M. Özcürümez, M. Orth, and T. Streichert, Age and Sex Dependent Reference Intervals for Random Plasma/Serum Glucose Concentrations Related to Different Sampling Devices and Determined by an Indirect Procedure with Data Mining. *J. Lab. Med.* 45, 95 (2021).

3. A.S. Bolla and R. Priefer, Blood Glucose Monitoring—An Overview of Current and Future Non-invasive Devices. *Diabetes Metab. Syndr.: Clin. Res. Rev.* 14, 739–751 (2020).

4. Z. Zhu, L. Garcia-Gancedo, A.J. Flewitt, H. Xie, F. Moussy, and W.I. Milne, A Critical Review of Glucose Biosensors Based on Carbon Nanomaterials: Carbon Nanotubes and Graphene. *Sensors* 12, 5996 (2012).

5. B. Zhu, X. Li, L. Zhou, and B. Su, An Overview of Wearable and Implantable Electrochemical Glucose Sensors. *Electroanalysis* 34, 237 (2021).

6. M. Falk, C. Psotta, S. Cirovic, and S. Shleev, Non-invasive Electrochemical Biosensors Operating in Human Physiological Fluids. *Sensors* 20, 6352 (2020).

7. J. Moyer, D. Wilson, I. Finkelshtein, B. Wong, and R. Potts, Correlation Between Sweat Glucose and Blood Glucose in Subjects with Diabetes. *Diabetes Technol. Ther.* 14, 398 (2012).

8. H. Karimi-Maleh, F. Karimi, M. Alizadeh, and A.L. Sanati, Electrochemical Sensors, A Bright Future in the Fabrication of Portable Kits in Analytical Systems. *Chem. Rec.* 20, 682 (2020).

9. H. Lee, Y.J. Hong, S. Baik, T. Hyeon, and D.H. Kim, Enzyme-Based Glucose Sensor: From Invasive to Wearable Device. *Adv. Healthc. Mater.* 7, 1701150 (2018).

10. T. Bobrowski and W. Schuhmann, Long-Term Implantable Glucose Biosensors. *Curr. Opin. Electrochem.* 10, 112 (2018).

11. S. Sharma, R. Kumari, S.K. Varshney, and B. Lahiri, Optical Biosensing with Electromagnetic Nanostructures. *Rev. Phys.* 5, 100044 (2020).

12. B.C. Satishkumar, L.O. Brown, Y. Gao, C.C. Wang, H.L. Wang, and S.K. Doorn, Reversible Fluorescence Quenching in Carbon Nanotubes for Biomolecular Sensing. *Nat. Nanotechnol.* 2, 560 (2007).

13. A. Camarca, A. Varriale, A. Capo, A. Pennacchio, A. Calabrese, C. Giannattasio, C. Murillo Almuzara, S. D'Auria, and M. Staiano, Emergent Biosensing Technologies Based on Fluorescence Spectroscopy and Surface Plasmon Resonance. *Sensors* 21, 906 (2021).

14. K. Wu, D. Su, Y. Feng, and J.P. Wang, 13. Magnetic Nanoparticle-Based Biosensing, in *Clinical Applications of Magnetic Nanoparticles: From Fabrication to Clinical Applications* (2018), p. 247

15. S.B. Matt, S. Raghavendra, M. Shivanna, M. Sidlinganahalli, and D.M. Siddalingappa, Electrochemical Detection of Paracetamol by Voltammetry Techniques Using Pure Zirconium Oxide

Nanoparticle Based Modified Carbon Paste Electrode. *J. Inorg. Organomet. Polym. Mater.* 31, 511 (2021).

16. S. Kim, K.H. Lee, J.Y. Lee, K.K. Kim, Y.H. Choa, and J.H. Lim, Single-Walled Carbon Nanotube-Based Chemi-Capacitive Sensor for Hexane and Ammonia. *Electron. Mater. Lett.* 15, 712 (2019).

17. H. Schlicke, S.C. Bittinger, H. Noei, and T. Vossmeyer, Gold Nanoparticle-Based Chemiresistors: Recognition of Volatile Organic Compounds Using Tunable Response Kinetics. *ACS Appl. Nano Mater.* 4, 10399 (2021).

18. G.A. Naikoo, T. Awan, H. Salim, F. Arshad, I.U. Hassan, M.Z. Pedram, W. Ahmed, H.L. Faruck, A.A. Aljabali, V. Mishra, and Á. Serrano-Aroca, Fourth-Generation Glucose Sensors Composed of Copper Nanostructures for Diabetes Management: A Critical Review. *Bioeng. Trans. Med.* 7, e10248 (2021).

19. Q. Li, J. Sheng, Q. Wei, Q. An, X. Wei, P. Zhang, and L. Mai, A Unique Hollow Li 3 Vo 4/Carbon Nanotube Composite Anode for High-rate Long-Life Lithium-Ion Batteries. *Nanoscale* 6, 11072 (2014).

20. Y. Dong, K. Md, Y.S. Chui, Y. Xia, C. Cao, J.M. Lee, and J.A. Zapien, Synthesis of CNT@ Fe$_3$O$_4$-C Hybrid Nanocables as Anode Materials with Enhanced Electrochemical Performance for Lithium-Ion Batteries. *Electrochim. Acta* 176, 1332 (2015).

21. P. Chakraborty, S. Dhar, N. Deka, K. Debnath, and S.P. Mondal, Non-enzymatic Salivary Glucose Detection Using Porous CuO Nanostructures. *Sensor Actuat. B-Chem.* 302, 127134 (2020).

22. P. Cui and A.J. Wang, Synthesis of CNTs/CuO and its Catalytic Performance on the Thermal Decomposition of Ammonium Perchlorate. *J. Saudi Chem. Soc.* 20, 343–348 (2016).

23. S. Paramparambath, S. Shafath, M.R. Maurya, J.J. Cabibihan, A.K. Al-Ali, R.A. Malik, and K.K. Sadasivuni, Nonenzymatic Electrochemical Sensor Based on CuO-MgO Composite for Dopamine Detection. *IEEE Sens. J.* 21, 25597 (2021).

24. J. Talla, M. Abusini, K. Khazaeleh, R. Omari, M. Serhan, and H. El-Nasser, Tuning Electronic Properties and Band Gap Engineering of Defective Carbon Nanotube Bundles: First Principles Calculations. *Mater. Express* 7, 516 (2017).

25. M.R. Maurya, V. Toutam, and D. Haranath, Comparative Study of Photoresponse from Vertically Grown ZnO Nanorod and Nanoflake Films. *ACS Omega* 2, 5538 (2017).

26. G.D. Park and Y.C. Kang, Multiroom-Structured Multicomponent Metal Selenide-Graphitic Carbon-Carbon Nanotube Hybrid Microspheres as Efficient Anode Materials for Sodium-Ion Batteries. *Nanoscale* 10, 8125 (2018).

27. X. Wang, B. Xia, X. Zhu, J. Chen, S. Qiu, and J. Li, Controlled Modification of Multiwalled Carbon Nanotubes with Zno Nanostructures. *J. Solid State Chem.* 181, 822 (2008).

28. S.M. Abbas, S.T. Hussain, S. Ali, F. Abbas, N. Ahmad, N. Ali, and Y. Khan, One-Pot Synthesis of A Composite of Monodispersed CuO Nanospheres on Carbon Nanotubes as Anode Material for Lithium-Ion Batteries. *J. Alloys Compd.* 574, 221 (2013).

29. K. Lokesh, G. Kavitha, E. Manikandan, G.K. Mani, K. Kaviyarasu, J.B.B. Rayappan, R. Ladchumananandasivam, J.S. Aanand, M. Jayachandran, and M. Maaza, Effective Ammonia Detection Using n-ZnO/p-NiO Heterostructured Nanofibers. *IEEE Sens. J.* 16, 2477 (2016).

30. J. Liang, J. Jiang, M. Xu, X. Huo, D. Ye, S. Zhang, X. Wu, and W. Wu, Improved Lithium Storage Performance of Urchin-Like CuO Microspheres by Stereotaxically Constructed Graphene Mediating Synergistic Effect. *J. Mater. Sci. Mater. Electron.* 32, 8557 (2021).

31. N.F. Khusnun, A.A. Jalil, S. Triwahyono, C.N.C. Hitam, N.S. Hassan, F. Jamian, W. Nabgan, T.A.T. Abdullah, M.J. Kamaruddin, and D. Hartanto, Directing the Amount of CNTs in CuO-CNT Catalysts for Enhanced Adsorption-Oriented Visible-Light-Responsive Photodegradation of p-Chloroaniline. *Powder Technol.* 327, 170 (2018).

32. D.K. Singh, S. Mohan, V. Kumar, and S.H. Hasan, Kinetic, Isotherm and Thermodynamic Studies of Adsorption Behaviour of CNT/CuO Nanocomposite for the Removal of as (III) and as (V) from Water. *RSC Adv.* 6, 1218 (2016).

33. K. Dhara and D.R. Mahapatra, Electrochemical Nonenzymatic Sensing of Glucose Using Advanced Nanomaterials. *Microchim. Acta* 185, 1 (2018).

34. Z. Amirzadeh, S. Javadpour, M.H. Shariat, and R. Knibbe, Nonenzymatic Glucose Sensor Based on Copper Oxide and Multi-wall Carbon Nanotubes Using PEDOT: PSS Matrix. *Synth. Met.* 245, 160 (2018).

35. J. Yang, Q. Lin, W. Yin, T. Jiang, D. Zhao, and L. Jiang, A Novel Nonenzymatic Glucose Sensor Based on Functionalized PDDA-Graphene/CuO Nanocomposites. *Sensor Actuat. B-Chem.* 253, 1087 (2017).

36. Y. Liu, J. Zhang, Y. Cheng, and S.P. Jiang, Effect of Carbon Nanotubes on Direct Electron Transfer and Electrocatalytic Activity of Immobilized Glucose Oxidase. *ACS Omega* 3, 667 (2018).

37. N. Abraham, R.R. Krishnakumar, C. Unni, and D. Philip, Simulation Studies on the Responses of ZnO-CuO/CNT Nanocomposite-Based SAW Sensor to Various Volatile Organic Chemicals. *J. Sci.: Adv. Mater. Devices* 4, 125 (2019).

38. X.H. Niu, L.B. Shi, H.L. Zhao, and M.B. Lan, Advanced Strategies for Improving the Analytical Performance of Pt-Based Nonenzymatic Electrochemical Glucose Sensors: A Minireview. *Anal. Methods* 8, 1755 (2016).

39. B.K. Shrestha, R. Ahmad, S. Shrestha, C.H. Park, and C.S. Kim, In Situ Synthesis of Cylindrical Spongy Polypyrrole Doped Protonated Graphitic Carbon Nitride for Cholesterol Sensing Application. *Biosens. Bioelectron.* 94, 686 (2017).

40. P.K. Sonkar, V. Ganesan, Metal Oxide-Carbon Nanotubes Nanocomposite-Modified Electrochemical Sensors for Toxic Chemicals, in *Metal Oxides in Nanocomposite-Based Electrochemical Sensors for Toxic Chemicals* (2021), pp. 235–261

41. M. Hassan, C. Vyas, B. Grieve, and P. Bartolo, Recent Advances in Enzymatic and Non-enzymatic Electrochemical Glucose Sensing. *Sensors* 21, 4672 (2021).

42. A. Savk, H. Aydın, K. Cellat, and F. Sen, A Novel High Performance Non-enzymatic Electrochemical Glucose Biosensor Based on Activated Carbon-Supported Pt-Ni Nanocomposite. *J. Mol. Liq.* 300, 112355 (2019).

43. X. Gao, X. Du, D. Liu, H. Gao, P. Wang, and J. Yang, Core-Shell Gold-Nickel Nanostructures as Highly Selective and Stable Nonenzymatic Glucose Sensor for Fermentation Process. *Sci. Rep.* 10, 1365 (2020).

44. H. Abunahla, B. Mohammad, A. Alazzam, M. Abi Jaoude, M. Al-Qutayri, S.A. Hadi, and S.F. Al-Sarawi, Momsense: Metal-Oxide-Metal Elementary Glucose Sensor. *Sci. Rep.* 9, 1 (2019).

45. J. Zhang, Y. Sun, X. Li, and J. Xu, Fabrication of Porous NiMn$_2$O$_4$ Nanosheet Arrays on Nickel Foam as an Advanced Sensor Material for Non-enzymatic Glucose Detection. *Sci. Rep.* 9, 1 (2019).

46. J. Qian, Y. Wang, J. Pan, Z. Chen, C. Wang, J. Chen, and Z. Wu, Non-enzymatic Glucose Sensor Based on ZnO-CeO$_2$ Whiskers. *Mater. Chem. Phys.* 239, 12205 (2020).

47. X. Gong, Y. Gu, F. Zhang, Z. Liu, Y. Li, G. Chen, and B. Wang, High-Performance Non-enzymatic Glucose Sensors Based on CoNiCu Alloy Nanotubes Arrays Prepared by Electrodeposition. *Front. Mater.* 6, 3 (2019).

48. J. Salifu, L. Tian, Y. Wang, WLu. Luo, and X. Sun, Self-assembled Graphene Platelet-Glucose Oxidase Nanostructures for Glucose Biosensing. *Biosens. Bioelectron.* 26, 4491 (2011).

49. S. Hu and C. Hu, Carbon Nanotube-Based Electrochemical Sensors: Principles and Applications in Biomedical Systems. *J. Sens.* (2009). https://doi.org/10.1155/2009/187615.

50. Q. Peng, Y. Zhang, S. Yang, T. Yuwen, Y. Liu, J. Fan, and G. Zang, Glucose Determination Behaviour of Gold Microspheres-Electrodeposited Carbon Cloth Flexible Electrodes in Neutral Media. *Anal. Chim. Acta* 1159, 338442 (2021).

51. A. Kundu and T.S. Fisher, Harnessing the Thermogalvanic Effect of the Ferro/Ferricyanide Redox Couple in A Thermally Chargeable Supercapacitor. *Electrochim. Acta* 281, 357 (2018).

52. S. Ghosh, T. Mathews, B. Gupta, A. Das, N.G. Krishna, and M. Kamruddin, Supercapacitive Vertical Graphene Nanosheets in Aqueouselectrolytes. *Nano-Struct. Nano-Objects* 10, 42 (2017).

53. L. Xu, Y. Zhu, X. Yang, and C. Li, Amperometric Biosensor Based on Carbon Nanotubes Coated with Polyaniline/Dendrimer-Encapsulated Pt Nanoparticles for Glucose Detection. *Mater. Sci. Eng. C* 29, 1306 (2009).

54. L. Xu, Y. Zhu, L. Tang, X. Yang, and C. Li, Biosensor Based on Self-Assembling Glucose Oxidase and Dendrimer-Encapsulated Pt Nanoparticles on Carbon Nanotubes for Glucose Detection. *Electroanalysis* 19, 717 (2007).

55. X. Tang, B. Zhang, C. Xiao, H. Zhou, X. Wang, and D. He, Carbon Nanotube Template Synthesis of Hierarchical $NiCoO_2$ Composite for Non-enzyme Glucose Detection. *Sens. Actuators B: Chem.* 222, 232 (2016).

56. V. Mani, B. Devadas, and S. Chen, Direct Electrochemistry of Glucose Oxidase at Electrochemically Reduced Graphene Oxide-Multiwalled Carbon Nanotubes Hybrid Material Modified Electrode for Glucose Biosensor. *Biosens. Bioelectron.* 41, 309 (2013).

57. X. Pang, D. He, S. Luo, and Q. Cai, An amperometric Glucose Biosensor Fabricated with Pt Nanoparticle-Decorated Carbon Nanotubes/TiO_2 Nanotube Arrays Composite. *Sens. Actuators B: Chem* 137, 134 (2009).

58. C. Lee, S. Lee, M. Cho, and Y. Lee, Nonenzymatic Amperometric Glucose Sensor Based on A Composite Prepared from Cuo, Reduced Graphene Oxide, and Carbon Nanotube. *Microchim. Acta* 183, 3285 (2016).

59. K. Hwa and B. Subramani, Synthesis of Zinc Oxide Nanoparticles on Graphene-Carbon Nanotube Hybrid for Glucose Biosensor Applications. *Biosens. Bioelectron.* 62, 127 (2014).

60. D. Pan, J. Chen, S. Yao, W. Tao, and L. NIE, An Amperometric Glucose Biosensor Based on Glucose Oxidase Immobilized in Electropolymerized Poly(O-Aminophenol) and Carbon Nanotubes Composite Film on A Gold Electrode. *Anal. Sci.* 21, 367 (2005).

61. W. Qin, X. Li, Y. Zhang, L. Han, Z. Cheng, Z. Li, and Y. Xu, Rational Design of Ag Nanoparticles on Zif-67-Functionalized Carbon Nanotube for Enzymeless Glucose Detection and Electrocatalytic Water Oxidation. *SSRN Electron. J.* 910, 164878 (2022).

62. S. Mohammadi, A. Taheri, and Z. Rezayati-Zadorcid, Ultrasensitive and Selective Non-enzymatic Glucose Detection Based On Pt Electrode Modified by Carbon Nanotubes@ Graphene Oxide/ Nickel Hydroxide-Nafion Hybrid Composite in Alkaline Media. *Progress Chem. Biochem. Res.* 1, 1 (2018).

63. L. Zou, S. Wang, and J. Qiu, Preparation and Properties of A Glucose Biosensor Based on An Ionic Liquid-Functionalized Graphene/Carbon Nanotube Composite. *New Carbon Mater.* 35, 12 (2020).

64. R. Devasenathipathy, V. Mani, S. Chen, S. Huang, T. Huang, C. Lin, K. Hwa, T. Chen, and B. Chen, Glucose Biosensor Based on Glucose Oxidase Immobilized at Gold Nanoparticles Decorated Graphene-Carbon Nanotubes. *Enzyme Microb. Technol.* 78, 40 (2015).

65. G. Luque, N. Ferreyra, and G. Rivas, Glucose Biosensor Based on the Use of a Carbon Nanotube Paste Electrode Modified with Metallic Particles. *Microchim. Acta* 152, 277 (2005).